

Reducing thermal transport in electrically conducting polymers: Effects of ordered mixing of polymer chains

Souvik Pal, Ganesh Balasubramanian, and Ishwar K. Puri

Citation: *Applied Physics Letters* **102**, 023109 (2013); doi: 10.1063/1.4776676

View online: <http://dx.doi.org/10.1063/1.4776676>

View Table of Contents: <http://scitation.aip.org/content/aip/journal/apl/102/2?ver=pdfcov>

Published by the **AIP Publishing**

Instruments for advanced science

Gas Analysis



- dynamic measurement of reaction gas streams
- catalysis and thermal analysis
- molecular beam studies
- dissolved species probes
- fermentation, environmental and ecological studies

Surface Science



- UHV TPD
- SIMS
- end point detection in ion beam etch
- elemental imaging - surface mapping

Plasma Diagnostics



- plasma source characterization
- etch and deposition process reaction kinetic studies
- analysis of neutral and radical species

Vacuum Analysis



- partial pressure measurement and control of process gases
- reactive sputter process control
- vacuum diagnostics
- vacuum coating process monitoring

contact Hiden Analytical for further details

HIDEN
ANALYTICAL

info@hideninc.com
www.HidenAnalytical.com

CLICK to view our product catalogue 

Reducing thermal transport in electrically conducting polymers: Effects of ordered mixing of polymer chains

Souvik Pal,¹ Ganesh Balasubramanian,² and Ishwar K. Puri^{1,a)}

¹Department of Engineering Science and Mechanics, Virginia Tech, Blacksburg, Virginia 24061, USA

²Department of Mechanical Engineering, Iowa State University, Ames, Iowa 50011, USA

(Received 20 November 2012; accepted 31 December 2012; published online 17 January 2013)

Reducing the phonon thermal conductivity of electrically conducting polymers can facilitate their use as potential thermoelectric materials. Thus, the influence of the coupling between the longitudinal and transverse phonon modes on overall thermal conductivity is explored for binary mixtures of polyaniline (PANI) and polyacetylene (PA) chains by considering various geometric polymer mixture configurations. The molecular simulations reveal that an increase in the interfacial area available for transverse interactions between dissimilar chains enhances atomic interactions that are orthogonal to the heat transfer direction. As transverse collisions between PA and PANI chains are enhanced, the motion of longitudinal phonons is disrupted, impeding thermal transport. This enhances phonon scattering and reduces longitudinal thermal transport. While there is a nonlinear decrease in the phonon thermal conductivity with increasing interfacial contact area, there is a corresponding linear growth in the nonbonded interaction energies between the different polymers. © 2013 American Institute of Physics. [<http://dx.doi.org/10.1063/1.4776676>]

Electrically conducting (EC) polymers such as polyacetylene (PA) and polyaniline (PANI) conduct electric current by moving delocalized electrons¹ associated with the sp^2 hybridized carbon atoms of the polymer chain backbone. This feature, coupled with their low thermal conductivity κ , makes them suitable for potential thermoelectric applications.^{2,3} The performance of a thermoelectric material is evaluated through its figure of merit ZT that is inversely proportional to κ . Strategies to manipulate κ facilitate the on demand tuning of ZT . Since electronic motion in EC polymers is different from the free electron drift observed in metals, energy, and charge transport through PANI and PA are only weakly correlated.^{2,4} Atomic vibrations (phonons) and interatomic collisions are the major thermal energy carriers in these polymers. Hence, by reducing the phonon contribution to the thermal conductivity κ_p , κ can be lowered considerably, which in turn enhances ZT .

While various strategies have been investigated to increase κ_p ,⁵⁻⁷ only a few studies have considered possibilities for its reduction.^{8,9} Unlike crystalline materials, polymer chains exhibit nonlinear anharmonic bonded interactions⁸ so that phonon transport through them is strongly dependent on the orientations of their backbone relative to the direction of heat transfer.^{6,9} Polymer chains that are more aligned along this direction offer a smaller resistance to phonon transport. Destroying such an ordered orientation by imposing mechanical strain or mixing dissimilar polymers increases phonon scattering and atomic collisions, and limits the phonon mean free paths, all of which reduce κ_p .⁹

Longitudinal phonon transport is coupled with transport in the transverse direction.¹⁰ In this Letter, we investigate the effect of this coupling in EC polymers and explore its applicability for reducing κ_p . We contend that

enhancing transverse phonon scattering across an interface that is placed parallel to the longitudinal direction of heat transfer should impede transport in this direction, lowering κ_p . Various binary PANI-PA polymer mixtures in various geometric configurations are selected to validate this hypothesis using atomistic simulations. Although it is understood how interfacial thermal resistance reduces κ_p in superlattice nanostructures,¹¹ discussions of the influence of transverse phonon scattering on κ_p are absent from the literature.

Nonequilibrium molecular dynamics (NEMD) simulations are employed to determine the thermal conductivity of the PANI-PA configurations using LAMMPS.¹² The term *interfacial area* S denotes the contact area between PANI and PA molecules. Four differently ordered PANI-PA binary polymer combinations are created. These have dissimilar S but the same 1:1 mixture ratio for the numbers of PANI-PA polymer chains. Combinations containing a random distribution of PANI and PA chains as well as those with pure polymers (or 1:0 and 0:1 mixture ratios) are also prepared. Each configuration has a cuboidal geometry of ΔX nm \times ΔY nm \times ΔZ nm consisting of 64 chains of each of PANI and PA. The geometrical details of these structures, including the values of ΔX , ΔY , and ΔZ for each configuration, are available in the supplementary material.¹³ The volume $V = \Delta X \Delta Y \Delta Z$ for all configurations at a specific temperature is comparable (with variation of $\sim 1\%$ from the mean value). Each polymer chain containing 24 carbon atoms is constructed as a linearly stretched entity that is aligned along the longitudinal direction of heat transfer x . The structures are generated with Xenoview.¹⁴ The parameters for the PCFF (polymer consistent force field) that describe the bonded and nonbonded interactions for these EC polymers are obtained from the literature.^{14,15} Details of the forcefield functions are described elsewhere.^{9,16} For all simulations, periodic boundary conditions are imposed along all three coordinate

^{a)} Author to whom correspondence should be addressed. Email: ikpuri@vt.edu. Tel.: +1-540-231-3243. Fax: +1-540-231-4574.

directions. The VMD package¹⁷ is used to visualize the simulated structures.

First, energy minimization is performed for each configuration using the conjugate gradient technique.¹² The details of the convergence of energy minimization are provided in the supplementary material.¹³ The minimized structure is then initialized at the simulation temperature (150, 200, 250, 300, 350, and 400 K for the different cases). This is followed by a two-step process where the configuration is: (1) first heated for 0.1 nanoseconds (ns) to a temperature much higher than the polymer glass transition temperature T_g , i.e., from $T=300$ K to $T=700$ K (for PANI, $T_g=493$ K, for PA, $T_g=473$ K), and (2) then cooled back to 300 K over 0.1 ns under a canonical (NVT) ensemble using a Langevin thermostat with a coupling time of 0.1 picoseconds (ps). This annealing and tempering relaxes the molecules and removes bond symmetries that could have been artifacts of polymer construction. Next, the configuration is equilibrated under an isothermal-isobaric ensemble (NPT) with $T=300$ K and $P=1$ atm. where the pressure is controlled by Nosé-Hoover barostat with a coupling time of 1 ps, followed by simulations under the NVT and NVE ensembles, each for 0.2 ns, respectively. Upon equilibration, the configuration relaxes to its appropriate mixture density. All simulations use a time-step of 0.001 ps.

The longitudinal κ_p is obtained by implementing the reverse NEMD technique.¹⁸ Along the x -wise direction, the exchange of kinetic energies between the coldest atoms in a 0.8950 (x) Å \times 43.16 (y) Å \times 36.99 (z) Å region, which serves as a heat source in the middle of the domain, with the hottest atoms at the two corresponding x -wise boundary regions (that serve as heat sinks with half the thickness of the heat source) provides the heat flux. Figure 1 schemati-

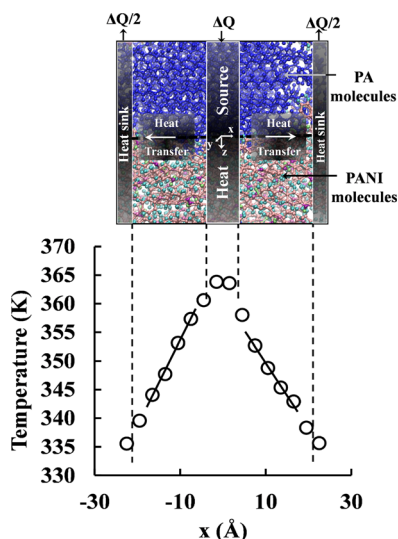


FIG. 1. The top panel illustrates the x - z cross sectional view of configuration 1 described in the supplementary material. The heat flux Q from the source is transferred along the x direction through the polymer mixture to the sinks at its two x -wise boundaries. The bottom panel presents the simulated temperature profile averaged over 10 samples recorded at regular intervals during the last 1 ns of reverse NEMD simulation. The linear portions of the temperature profiles are used to calculate the average temperature gradient. The locations of the peak temperature(s) correspond to the heat source in the top panel, while the lower temperatures at both boundaries correspond to the two heat sinks.

cally illustrates the direction of heat transfer and shows the steady state temperature distribution along x direction of the polymer configuration 1. After the heat transfer reaches steady state, the temperature distribution is sampled over data recorded every 100 ps during the last 1 ns of the 5 ns long NEMD simulations. Temperature gradients are calculated from the linear portions of the temperature distribution for all the recorded data, and a steady state value is obtained from a temporal average over these gradients. The net steady state heat flux transferred from the heat source to the sinks is also determined from a temporal average. Finally, κ_p is calculated using Fourier's heat conduction law.¹⁹

We use κ_{pn} to denote the value of κ_p normalized with respect to κ_p^{PANI} at the corresponding temperature. At room temperature (300 K), κ_p^{PANI} is $0.135 \text{ Wm}^{-1} \text{ K}^{-1}$, a value that is obtained by simulating only PANI chains contained in the reference cuboid. Likewise, we calculate $\kappa_p^{PA} = 0.088 \text{ Wm}^{-1} \text{ K}^{-1}$ at $T=300$ K. For each binary mixture, S (and surface area to volume ratio S/V) is obtained by examining the cross section (in y - z plane) of the domain taken at the lower boundary of x -axis and multiplying the length of the interface by the domain length along x -wise direction. As described in the supplementary material,¹³ we use an image analysis scheme to identify visually ill-defined contact regions. For a given chain ratio, the random distribution provides the largest S .

Figure 2 shows the variation of κ_{pn} with respect to PANI-PA interfacial area at $T=300$ K for identical (1:1) chain ratios. As S/V increases, κ_{pn} decreases. While a typical mixture rule predicts a single value of κ_p ,^{9,20} it is instead evident from Fig. 2 that the thermal transport and the conductivity also depend upon the polymer mixture configurations and the magnitudes of their interfacial contact areas. Different configurations alter the magnitude of the transverse interactions between the PANI and PA chains. Increasing the interfacial contact area between these two chains increases

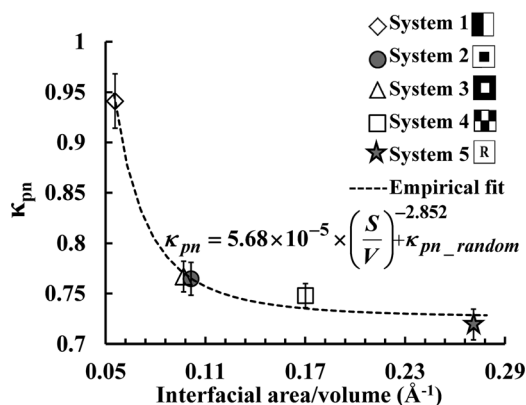


FIG. 2. The variation of the normalized thermal conductivity κ_{pn} (κ_p/κ_p^{PANI}) with the interfacial contact area per unit volume (S/V) between PANI-PA chains at $T=300$ K. The different markers correspond to the binary PANI-PA configurations whose cross sectional configurations are schematically illustrated in the figure legend. Each such schematic reflects the cross sectional (yz plane) view of the binary mixture, perpendicular to the direction (x) of heat transfer, where black represents PANI, white PA, and R a random distribution of PANI and PA. Error bars denote the standard error in κ_p calculated from ten spatially averaged temperature profiles at intervals of 0.1 ns over the last 1 ns of the simulation and normalized with respect to κ_p^{PANI} . An empirical fit that asymptotically reaches a limiting value of κ_{pn} shows that $\kappa_{pn} - \kappa_{pn,random} \propto \left(\frac{S}{V}\right)^{-2.852}$.

phonon scattering through enhanced atomic collisions. This reduces κ_p for the ordered polymer mixture from that of the pure material κ_p^{PANI} so that $\kappa_{pn} < 1$. Thus, stronger interfacial interactions lead to smaller κ_{pn} , which reveal that the higher energy losses due to transverse phonon interactions (or scattering) impede longitudinal thermal transport. The higher transverse scattering decreases the phonon mean free paths, thereby lowering longitudinal κ_p . This validates our conjecture that there is a mode coupling between phonons along the transverse and longitudinal directions even for noncrystalline polymer configurations. Since S/V increases with diminishing length scale, the effects of these transverse interactions become more pronounced at the nanoscale.

Empirically, we find

$$\kappa_{pn} = 5.68 \times 10^{-5} \times \left(\frac{S}{V}\right)^{-2.852} + \kappa_{pn,random}. \quad (1)$$

This fit reaches an asymptotic value for κ_{pn} , implying that beyond a certain threshold interfacial area (provided by a random mixing of polymers), κ_p cannot be lowered any further through polymer mixing. It follows from Eq. (1) that $\kappa_{pn} - \kappa_{pn,random} \propto \left(\frac{S}{V}\right)^{-2.852}$.

For amorphous polymers, the dependence of κ on temperature is different below and above the glass transition temperature.²¹ Below T_g , the thermal conductivity increases with temperature due to the reduction in polymer chain entanglement that lowers energy scattering at chain bends. Close to T_g or above it, chain mobility increases as the polymers undergo large movements, thereby creating voids that scatter phonons and lower κ . The thermal conductivities of PANI and PA also increase below T_g with increasing temperature because of enhanced specific heat.^{22,23}

Figure 3 presents the variation of κ_{pn} and κ_p^{PANI} for configurations 1 and 4, described in the supplementary material,¹³ at different temperatures. κ_p^{PANI} increases with temperature up to 300 K and then slightly decreases close to T_g (493 K), suggesting an increase in phonon scattering from emerging defects in form of voids. In contrast, κ_{pn} for configuration 1 decreases continually with increasing T , implying that interfacial interatomic interactions and collisions

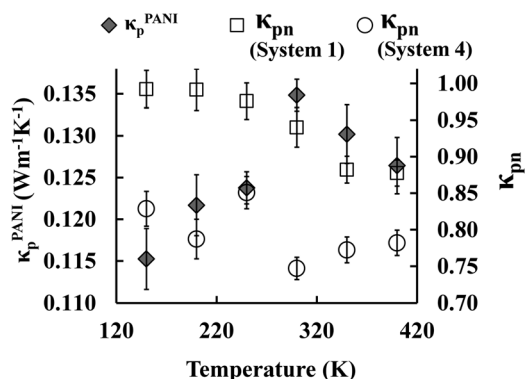


FIG. 3. The evolution of κ_{pn} for configurations 1 and 4 and κ_p^{PANI} as a function of temperature. Here, κ_p^{PANI} is the thermal conductivity of a configuration with only PANI chains. Error bars are determined as described in Fig. 2. For κ_{pn} , error bars at different temperatures are normalized with respect to κ_p^{PANI} at the corresponding temperature, whereas for κ_p^{PANI} , they are in units of $\text{Wm}^{-1}\text{K}^{-1}$.

increase at higher temperatures. However, for the relatively more complex mixture configuration 4 that has larger S , κ_p does not vary as significantly with temperature. Thus, we conjecture that the reduction in κ_p due to transverse phonon scattering is characteristic of a simple ordered mixture configuration and relatively small S .

Figure 4 shows the temperature dependent variation of κ_{pn} for the different binary mixture configurations as a function of S/V . For each configuration, both S and V increase by small amounts with temperature due to thermal expansion although the ratio S/V remains relatively unaltered (and lies within 2% for a particular configuration). For a specified temperature, κ_{pn} typically decreases with increasing S/V . While for configuration 1, κ_{pn} steadily decreases with increasing temperature in accord with Fig. 3, more complex mixing configurations with larger S and enhanced transverse phonon interactions do not exhibit an as organized temperature dependence for κ_{pn} .

We evaluate the interaction energies between the two different polymers for each configuration. The interaction energies of PANI molecules with the PA chains consist of *van der Waals* and *Coulombic* energy components. Since the volumes of the different configurations are comparable, Fig. 5 shows that the interaction energies increase with increasing S . The reduction in κ_{pn} with increases in S occurs due to the growth in the locations across, which different polymers are able to interact and subsequently scatter the energy transported by phonons and atomic collisions. While κ_{pn} is nonlinearly correlated with S/V as shown in Fig. 2, the interaction energies demonstrate a linear relationship with S/V .

Longitudinal thermal transport occurs due to delocalized phonons traveling along the x -direction as well the energy carried by atomic collisions along the same direction. Increasing S increases transverse interatomic and polymer interactions. These raise the potential energies associated with the *van der Waals* and *Coulombic* components, displacing phonons from their longitudinal trajectories, scattering their energies, and reducing κ_p . Thus, the greater the magnitude of the interaction energies between the PANI and PA

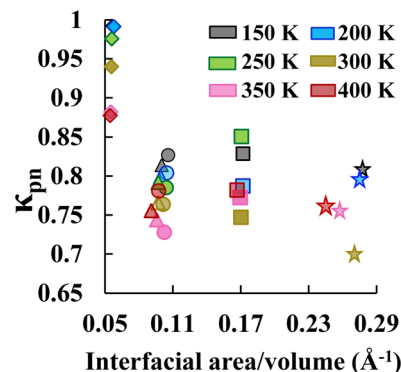


FIG. 4. The variation of κ_{pn} as a function of S/V between PANI-PA for different temperatures. The value at a specific temperature is obtained by normalizing κ_p with respect to κ_p^{PANI} at that temperature. Different colors represent the various temperatures while different markers denote the various mixture configurations similar to Fig. 2. The S/V values for a particular configuration, although comparable at different temperatures, are not equal because of small temperature dependent changes in S and V . Consequently, data points for the same configuration are not exactly vertically aligned.

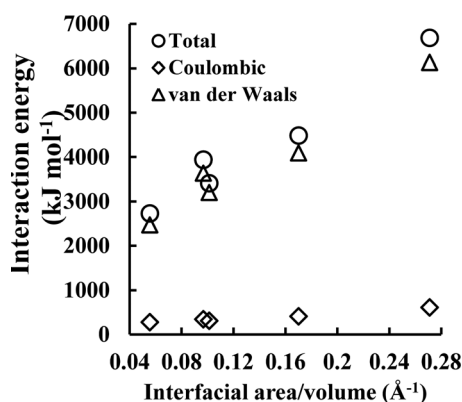


FIG. 5. The variation in interaction energies as a function of S/V . The total interaction energy between PANI and PA molecules consists of pairwise interaction and Coulombic energies that are also separately presented here. For all the simulated cases, absolute magnitudes of the energies are presented.

chains, the stronger is the impedance to phonon motion along the heat transfer direction (and the lower κ_p is).

In summary, the influence of transverse polymer interactions and interatomic collisions on the longitudinal heat transfer in binary mixtures of PANI and PA chains is investigated. Interfaces that lie parallel to the heat transfer direction reduce phonon thermal conductivity due to transverse phonon scattering. The intrinsic coupling of longitudinal and transverse vibrational modes in these polymers impedes longitudinal thermal transport. κ_{pn} has a nonlinear relationship with S/V . For simple mixing configurations that generate interfaces with relatively smaller interfacial areas, the enhancement of transverse phonon scattering with increasing temperature further reduces κ_p although such a temperature dependent trend does not hold for more complex configurations with larger interfacial areas. The underlying reason for the κ_p dependence on S/V is illustrated by the linear increase in the intermolecular interaction energies between the two sets of polymer chains with increasing S . The enhancement in the interaction energies is due to the increase in transverse polymer interactions and atomic collisions that perturb the longitudinal phonon paths, thereby impeding heat transfer

and lowering κ_p . Such a polymer mixing approach that lowers κ_p and increases ZT could facilitate the employment of PANI and PA for potential soft-thermoelectric applications requiring high thermal resistance.

S.P. thanks the Virginia Tech Department of Engineering Science and Mechanics for the use of their Linux Computing Cluster (LCC).

¹G. Inzelt, M. Pineri, J. W. Schultze, and M. A. Vorotyntsev, *Electrochim. Acta* **45**(15–16), 2403 (2000).

²J. Z. Jin, Q. Wang, and M. A. Haque, *J. Phys. D: Appl. Phys.* **43**(20), 205302 (2010).

³Y. W. Park, C. O. Yoon, C. H. Lee, H. Shirakawa, Y. Suezaki, and K. Akagi, *Synth. Met.* **28**(3), D27 (1989).

⁴C. Kittel, *Introduction to Solid State Physics* (Wiley, New York, 1966).

⁵A. Henry and G. Chen, *Phys. Rev. Lett.* **101**(23), 235502 (2008).

⁶J. Liu and R. G. Yang, *Phys. Rev. B.* **81**(17), 174122 (2010).

⁷S. Shen, A. Henry, J. Tong, R. Zheng, and G. Chen, *Nat. Nanotechnol.* **5**(4), 251 (2010).

⁸W. P. Hsieh, M. D. Losego, P. V. Braun, S. Shenogin, P. Keblinski, and D. G. Cahill, *Phys. Rev. B* **83**(17), 174205 (2011).

⁹S. Pal, G. Balasubramanian, and I. K. Puri, *J. Chem. Phys.* **136**(4), 044901 (2012).

¹⁰M. Alaghemandi, J. Schulte, F. Leroy, F. Müller-plathe, and M. C. Böhm, *J. Comput. Chem.* **32**(1), 121 (2011).

¹¹G. Balasubramanian and I. K. Puri, *Appl. Phys. Lett.* **99**(1), 013116 (2011).

¹²S. J. Plimpton, *J. Comput. Phys.* **117**(1), 1 (1995).

¹³See supplementary material at <http://dx.doi.org/10.1063/1.4776676> for geometrical details of different structures and interfacial area calculation.

¹⁴S. Shenogin and R. Ozisik, *Polymer* **46**(12), 4397 (2005).

¹⁵M. M. Ostwal, T. T. Tsotsis, and M. Sahimi, *J. Chem. Phys.* **126**(12), 124903 (2007).

¹⁶M. M. Ostwal, M. Sahimi, and T. T. Tsotsis, *Phys. Rev. E* **79**(6), 061801 (2009).

¹⁷W. Humphrey, A. Dalke, and K. Schulten, *J. Mol. Graphics Modell.* **14**(1), 33 (1996).

¹⁸F. Müller-Plathe, *J. Chem. Phys.* **106**(14), 6082 (1997).

¹⁹F. P. Incropera, *Fundamentals of Heat, Mass Transfer* (Wiley, N.J., 2007).

²⁰G. Balasubramanian, I. K. Puri, M. C. Böhm, and F. Leroy, *Nanoscale* **3**(9), 3714 (2011).

²¹P. Dashora and G. Gupta, *Polymer* **37**(2), 231 (1996).

²²P. B. Kaul, K. A. Day, and A. R. Abramson, *J. Appl. Phys.* **101**(8), 083507 (2007).

²³R. J. Schweizer, K. Menke, and S. Roth, *J. Chem. Phys.* **81**(12), 6301 (1984).